

# Bayesian design for minimising uncertainty in spatial processes

Senarathne SGJ<sup>\*1</sup>, Müller WG<sup>2</sup>, and McGree JM<sup>1</sup>

<sup>1</sup>School of Mathematical Sciences, Science and Engineering Faculty, Queensland University of Technology, Brisbane, Australia

<sup>2</sup>Department of Applied Statistics, Johannes Kepler University Linz, Austria

## ABSTRACT

Model-based geostatistical design involves the selection of locations to collect data to minimise an expected loss function over a set of all possible locations. The loss function is specified to reflect the aim of data collection, which, for geostatistical studies, would typically be to minimise the uncertainty in a spatial process. In this paper, we propose a new approach to design such studies via a loss function derived through considering the entropy of model predictions, and we show that this simultaneously addresses the goal of precise parameter estimation. One drawback of this loss function is that it is computationally expensive to evaluate, so we provide an efficient approximation such that it can be used within realistically sized geostatistical studies. To demonstrate our approach, we apply the proposed approach to design the collection of spatially dependent multiple responses, and compare this with either designing for estimation or prediction only. The results show that our designs remain highly efficient in achieving each experimental objective individually, and provide an ideal compromise between the two objectives. Accordingly, we advocate that our design approach should be used more generally in model-based geostatistical studies.

**Keywords:** Copula models, Entropy, Generalised linear mixed models, Multiple response models, Spatial dependence.

## 1 Introduction

The importance of spatial dynamics in natural processes has become a major focus of enquiry in many fields including ecology, agriculture and marine biology (Bloom and Kentwell, 1999; Bruno et al., 2001; Castrignanò et al., 2008; Falk et al., 2014). Often, what can be explored and ultimately inferred about such dynamics depends on how the data were collected, and, in particular, the specific locations in space (Müller, 2007). In this paper, we propose an approach in Bayesian design for selecting sampling locations to efficiently learn about the spatial dynamics underpinning natural processes. In particular, we focus on quantifying and minimising uncertainty about model predictions at unobserved locations, and show how this simultaneously yields precise estimates of parameters.

One common approach to modelling spatial dynamics is via a Gaussian process model (Diggle et al., 2003). Such a model assumes that the underlying spatial dynamics can be expressed

---

<sup>\*</sup>Corresponding author: jagath.gedara@hdr.qut.edu.au

as a realisation of an unobserved stationary Gaussian process  $\{S(\mathbf{d}); \mathbf{d} \in \mathbb{R}^2\}$ , where  $\mathbf{d}$  is the location of interest. This stationary process  $S(\cdot)$  is typically assumed to have a mean value  $\boldsymbol{\mu}$  and a covariance matrix  $\boldsymbol{\Sigma}$  such that  $S(\cdot) \sim N(\boldsymbol{\mu}, \boldsymbol{\Sigma})$ . Here, the covariance matrix  $\boldsymbol{\Sigma}$  is defined via a distance-based covariance function  $\text{Cov}(h) = \text{Cov}[S(\mathbf{d}), S(\mathbf{d}')] ]$ , where  $h = \|\mathbf{d} - \mathbf{d}'\|$  is the Euclidean distance between locations  $\mathbf{d}$  and  $\mathbf{d}'$ . Realisations from the spatial process will be denoted by  $y_i$ , with each  $y_i$  being conditionally independent given  $S(\mathbf{d}_i)$ , for  $i = 1, \dots, n$ . For ease of notation,  $S(\mathbf{d}_i)$  will be abbreviated by  $s_i$  throughout the remainder of this article. The potential influence of covariates  $\mathbf{X}_i$  also collected at location  $\mathbf{d}_i$  can be incorporated via a linear predictor, with a link function used to map the linear predictor to the space of the expected response. Through such a model, one can then leverage information about the spatial variability between locations to yield accurate predictions at unobserved locations.

Bayesian inference provides a rigorous framework to quantify and handle uncertainty in spatial predictions, and a number of authors have considered this framework to design geostatistical studies. The work of Diggle and Lophaven (2006) compared the prediction performance of different classes of designs such as the ‘lattice plus close pairs’ and ‘lattice plus in-fill’ designs under parameter uncertainty. As such, no optimisation of the design was undertaken. This is presumably because of the large computational time involved in evaluating their loss function, and this is typical of designs for prediction. A pseudo-Bayesian design approach was proposed by Falk et al. (2014) for sampling on stream networks. Optimal designs were found under various loss functions but their work was limited to assuming some or all parameter values were known *a priori*. Bayesian approaches to design monitoring networks were proposed by Müller et al. (2004) and Fuentes et al. (2007) such that accurate predictions could be obtained while minimising the cost of monitoring. However, both approaches do not take into account parameter uncertainty. Further, to form a dual-objective loss function, both approaches considered a linear combination of loss functions which requires specifying the relative importance of each objective via pre-defined weights. Unfortunately, such an approach has been shown to be difficult to apply in practice (Hill et al., 1968; Cook and Wong, 1994; McGree et al., 2008).

Across all of the methods proposed in the above cited papers, no approach has taken into account both parameter uncertainty and the uncertainty in the predicted outcomes when quantifying the uncertainty in a spatial process. This is potentially a major limitation as both sources of uncertainty could be significant. Further, all of these approaches were limited to consider spatially dependent univariate responses. This is potentially because of the difficulty in constructing a multivariate distribution that appropriately describes the dependencies between each response. As each response may be of a different type (i.e. continuous, count, binary, etc), this can lead to a rather complex model, rendering many approaches in Bayesian design computationally infeasible. Such a limitation seems rather restrictive as multiple responses are often observed in geostatistical studies e.g. Bohorquez et al. (2017); Musafer and Thompson (2017).

To address the limitations of previous research, we consider a generalised linear spatial modelling (GLSM) framework where the dependence between responses is described by a Copula model. Such a model is flexible in that a variety of different dependence structures can be described via the cumulative distribution of the response. Thus, different data types are handled straightforwardly. Then, given such a model, we propose to quantify the uncertainty in spatial predictions via an entropy-based loss function. The benefit of this is that one can then exploit the additivity property of entropy, avoiding the need to pre-specify weights on each objective. To demonstrate the value of this approach, we design a simulated and real-world geostatistical

study, and assess the performance of the resulting designs.

This paper is outlined as follows. In Section 2, the GLSM framework for modelling spatial outcomes is defined, and the Copula representation for describing multivariate spatial data is introduced. Our Bayesian design framework is described in Section 3, along with our approach to quantify and minimise uncertainty in model predictions. In doing so, we show how such an approach also minimises uncertainty about parameter estimates, and provide an approximation to efficiently evaluate this loss function. To illustrate our methodologies, Section 4 focuses on finding designs in two examples where bivariate mixed spatial outcomes are observed. The paper concludes with a discussion of key findings and suggestions for future research.

## 2 Modelling multiple responses in a geostatistical study

In this section, we describe our modelling framework for multiple responses collected in a geostatistical study. We start by first describing how a univariate response could be modelled, then extend to multiple responses.

### 2.1 Spatial model for a univariate response

To model a univariate response collected in a geostatistical study, we consider a GLSM which has the following form:

$$\mu_i = \mathbf{X}_i^T \boldsymbol{\beta} + s_i \quad \text{and} \quad E(y_i | s_i) = g^{-1}(\mu_i), \text{ for } i = 1, 2, \dots, n,$$

where  $\mathbf{X}_i = (1, X_{i1}, \dots, X_{ip-1})^T$  is the covariate vector associated with the location  $\mathbf{d}_i$ ,  $\boldsymbol{\beta} \in \mathbb{R}^p$  are the regression coefficients (fixed effects), and  $s_i$  is the value of the  $i^{th}$  random effect. Here, the link function  $g(\cdot)$  defines the relationship between the linear predictor  $\mu_i$  and the expected outcome given  $s_i$ .

The random effects  $s_i = \{S(\mathbf{d}_i); \mathbf{d}_i \in \mathbb{R}^2\}$  for  $i = 1, \dots, n$ , are assumed to form a zero-mean Gaussian random field with a covariance matrix  $\boldsymbol{\Sigma}$ . When estimating this covariance matrix, it is convenient to consider a specific parametric family of covariance functions ([Albert and McShane, 1995](#); [Diggle et al., 2003](#)). In this paper, the squared exponential covariance function is used, and has the following form:

$$Cov(h; \boldsymbol{\gamma}) = \begin{cases} \gamma_0 + \gamma_1 & \text{if } h = 0 \\ \gamma_1 \exp(-\frac{h^2}{2\gamma_2^2}) & \text{if } h \neq 0, \end{cases}$$

where  $\boldsymbol{\gamma} = (\gamma_0, \gamma_1, \gamma_2)$  and  $h$  is the Euclidean distance between two locations. The parameters  $\gamma_0$ ,  $\gamma_1$  and  $\gamma_2$  are the nugget effect, partial sill and the spatial range, respectively.

To describe a Bayesian framework for the above model, let  $\mathbf{y}_i = (y_{i1}, \dots, y_{in_i})^T$  denote the observed data at location  $\mathbf{d}_i$  where  $n_i$  is the number of observations collected at location  $\mathbf{d}_i$ , for  $i = 1, \dots, n$ . In spatial design, the design  $\mathbf{d} = (\mathbf{d}_1, \dots, \mathbf{d}_n)^T$  represents the locations where

the outcomes  $\mathbf{y} = (\mathbf{y}_1, \dots, \mathbf{y}_n)^T$  are measured. Let  $p(\boldsymbol{\theta})$  denote the prior distribution about the parameters  $\boldsymbol{\theta}$ . Then, within a Bayesian framework, all inferences are based on the posterior distribution defined as follows:

$$p(\boldsymbol{\theta}|\mathbf{y}, \mathbf{d}) \propto \prod_{i=1}^n \prod_{j=1}^{n_i} p(y_{ij}|\mathbf{d}_i, s_i, \boldsymbol{\beta}) p(\mathbf{s}|\boldsymbol{\gamma}) p(\boldsymbol{\theta}),$$

where  $\mathbf{s} = (s_1, \dots, s_n)^T$  is vector of random effects, and the parameter vector  $\boldsymbol{\theta}$  includes both model parameters  $\boldsymbol{\beta}$  and covariance parameters  $\boldsymbol{\gamma}$ .  $p(y_{ij}|\mathbf{d}_i, s_i, \boldsymbol{\beta})$  is the conditional likelihood of observing  $y_{ij}$  at location  $\mathbf{d}_i$  given the model parameters  $\boldsymbol{\beta}$  and random effects  $s_i$  for  $i = 1, \dots, n$  and  $j = 1, \dots, n_i$ .

To extend the above model to handle multiple responses, we consider Copula models to describe the dependence between responses (Nelsen, 2006) (see next section). Alternative approaches for modelling such data are available in the literature. In particular, Copula-based approaches have been used to describe spatial variability in geostatistical data (Bárdossy, 2006; Kazianka and Pilz, 2011; Grler and Pebesma, 2011). Of note, our modelling framework is more flexible than such an approach as the dependence between responses can have a different form to the dependence between locations.

## 2.2 Spatial model for multiple responses

Here, we define a modelling approach for our multiple spatial responses by combining the univariate spatial models (defined above) with a suitable Copula model. For this, assume that two response variables will be observed with one being continuous  $Y_1$  and the other being discrete  $Y_2$ ; thus marginally they can be explained using two GLSMs as follows:

$$\begin{aligned} \mu_{1i} &= \mathbf{X}_i^T \boldsymbol{\beta}_1 + s_{1i}, \quad E(y_{1i}|s_{1i}) = g_1^{-1}(\mu_{1i}), \quad \text{and} \\ \mu_{2i} &= \mathbf{X}_i^T \boldsymbol{\beta}_2 + s_{2i}, \quad E(y_{2i}|s_{2i}) = g_2^{-1}(\mu_{2i}) \quad \text{for } i = 1, 2, \dots, n. \end{aligned}$$

Further, we assume that  $Y_1$  and  $Y_2$  have marginal probability distributions  $f_{Y_1|s_{1i}}$  and  $f_{Y_2|s_{2i}}$  given the random effects  $s_{1i}$  and  $s_{2i}$ , respectively. Further, denote the marginal cumulative distribution function of  $Y_1|s_{1i}$  and  $Y_2|s_{2i}$  as  $F_{Y_1|s_{1i}}$  and  $F_{Y_2|s_{2i}}$ , respectively. Thus, the Copula representation of the joint distribution  $G_{Y_1|s_{1i}, Y_2|s_{2i}}$  is given by,

$$\begin{aligned} G_{Y_1|s_{1i}, Y_2|s_{2i}}(y_{1ij}, y_{2ij}) &= C(F_{Y_1|s_{1i}}(y_{1ij}), F_{Y_2|s_{2i}}(y_{2ij}); \alpha) \\ &= C(u_{1ij}, u_{2ij}; \alpha) \quad \text{for } i = 1, 2, \dots, n \text{ and for } j = 1, 2, \dots, n_i, \end{aligned}$$

where  $C$  and  $\alpha$  denote the Copula function and the Copula parameter, respectively.

Then, the Copula representation of the joint distribution of  $Y_1|s_{1i}$  and  $Y_2|s_{2i}$  is given by,

$$f_{Y_1|s_{1i}, Y_2|s_{2i}}(y_{1ij}, y_{2ij}) = f_{Y_1|s_{1i}}(y_{1ij})(c_{1ij} - c_{1ij}^*), \quad (1)$$

where  $c_{1ij} = \frac{\partial C(u_{1ij}, u_{2ij}; \alpha)}{\partial u_{1ij}}$ ,  $c_{1ij}^* = \frac{\partial C(u_{1ij}, u_{2ij}^-; \alpha)}{\partial u_{1ij}}$  and  $u_{2ij}^-$  is the left hand limit of  $u_{2ij}$ , see Joe (2014) and Tao et al. (2013) for further details.

Then, using Equation (1), the conditional likelihood of a bivariate mixed outcome ( $\mathbf{y} = (y_{1ij}, y_{2ij})$  for  $i = 1, 2, \dots, n$  and  $j = 1, 2, \dots, n_i$ ) can be expressed as follows:

$$p(\mathbf{y}|\mathbf{d}, \boldsymbol{\theta}, \mathbf{s}_1, \mathbf{s}_2) = \prod_{i=1}^n \prod_{j=1}^{n_i} \left[ (f_{Y_1|s_{1i}}(y_{1ij})) (c_{1ij} - c_{1ij}^*) \right],$$

where  $\boldsymbol{\theta}$  includes all the model parameters  $(\boldsymbol{\beta}_1, \boldsymbol{\beta}_2)$ , the covariance parameters  $(\boldsymbol{\gamma}_1, \boldsymbol{\gamma}_2)$ , and the Copula parameter  $\alpha$ .

The bivariate Copula function describes the dependence structure between two random variables. A large number of bivariate Copulas and their dependence properties have been discussed in the literature (Durante and Sempi, 2010; Genest and MacKay, 1986; Nelsen, 2006). Among them, the bivariate Archimedean Copula models such as Clayton, Gumbel and Frank Copulas have been widely used due to their flexibility in describing different tail behaviours and different dependence structures.

The Clayton Copula is considered later in this paper to model the joint distribution of the responses with the reader referred to Clayton (1978) and Cook and Johnson (1981) for further details. The choice of this Copula model was motivated by the tail dependence structure of the data observed in the motivating example and desirable properties of the Archimedean Copula family to which this Copula belongs. For example, as provided by Genest and MacKay (1986), there is a closed form relationship between the bivariate Archimedean Copula parameter and Kendall's tau ( $\tau$ ). Therefore, once the Copula parameter is estimated, it is straightforward to define the dependence between the two responses within the intuitive scale of  $-1$  to  $+1$ .

### 3 Bayesian design framework for geostatistical studies

Our aim of minimising the uncertainty in a spatial process can be quantified within a Bayesian design framework by a loss function which we will denote as  $\lambda(\mathbf{d}, \boldsymbol{\theta}, \mathbf{y})$ . Such a loss function compares a summary of the posterior distribution for  $\boldsymbol{\theta}$  (based on observing  $\mathbf{y}$  from  $\mathbf{d}$ ) with its true value. However, as this function depends on  $\boldsymbol{\theta}$  and  $\mathbf{y}$ , which are unknown *a priori*, it cannot be used to select designs. Accordingly, the expectation of the loss function is used to locate designs, and this expectation can be defined as follows:

$$L(\mathbf{d}) = E_{\mathbf{y}, \boldsymbol{\theta}}[\lambda(\mathbf{d}, \boldsymbol{\theta}, \mathbf{y})] = \int_{\mathbf{y}} \int_{\boldsymbol{\theta}} \lambda(\mathbf{d}, \boldsymbol{\theta}, \mathbf{y}) p(\mathbf{y}|\boldsymbol{\theta}, \mathbf{d}) p(\boldsymbol{\theta}) d\boldsymbol{\theta} d\mathbf{y}. \quad (2)$$

When the loss function does not depend on the model parameters  $\boldsymbol{\theta}$ , Equation (2) can alternatively be expressed as:

$$L(\mathbf{d}) = E_{\mathbf{y}}[\lambda(\mathbf{d}, \mathbf{y})] = \int_{\mathbf{y}} \lambda(\mathbf{d}, \mathbf{y}) p(\mathbf{y}|\mathbf{d}) d\mathbf{y}. \quad (3)$$

A Bayesian design is then found by minimising the expected loss over the space of all possible locations. However, in general, the expected loss function does not have a closed-form solution, and hence, needs to be approximated. Monte Carlo (MC) integration is the most commonly used approach for approximating the expected loss. This is achieved by generating a large number of prior predictive data sets, evaluating the loss function for each data set, and then taking the average as the approximation to the expected loss. Formally:

$$\hat{L}(\mathbf{d}) = \frac{1}{K} \sum_{k=1}^K \lambda(\mathbf{d}, \boldsymbol{\theta}_k, \mathbf{y}_k), \quad (4)$$

where  $\boldsymbol{\theta}_k$  and  $\mathbf{y}_k$  are generated from the distributions  $p(\boldsymbol{\theta})$  and  $p(\mathbf{y}|\mathbf{d}, \boldsymbol{\theta}_k)$ , respectively.

The current approach to Bayesian design for spatial prediction is based on a loss function proposed in Diggle and Lophaven (2006). This loss function quantifies the spatially averaged prediction variance of the unobserved random field  $S(\cdot)$  over the predicted region  $\mathcal{A}$  as follows:

$$\lambda_{pred}(\mathbf{d}, \mathbf{y}) = \int_{\boldsymbol{\xi} \in \mathcal{A}} \text{Var}\{S(\boldsymbol{\xi})|\mathbf{y}, \mathbf{d}\} d\boldsymbol{\xi}. \quad (5)$$

When the prediction region  $\mathcal{A}$  consists a discrete set of locations  $\boldsymbol{\xi}_1, \boldsymbol{\xi}_2, \dots, \boldsymbol{\xi}_T$ , the above loss function can be expressed as follows:

$$\lambda_{pred}(\mathbf{d}, \mathbf{y}) = \frac{1}{T} \sum_{t=1}^T \text{Var}\{S(\boldsymbol{\xi}_t)|\mathbf{y}, \mathbf{d}\}.$$

As discussed in Diggle and Lophaven (2006), this loss function provides some provision to also address the objective of parameter estimation, and we explore this through the motivating examples presented in this paper. In the next section, we describe an alternative approach for addressing these dual objectives.

### 3.1 An entropy-based loss function for spatial prediction

Here, we derive a loss function to quantify uncertainty in a spatial process by considering the entropy about the predictions. For this, we note that, for a given model, there are two sources of uncertainty about the predictions: (1) Uncertainty in the parameter values; and (2) Uncertainty in the predicted outcome  $\mathbf{Z}$  conditional on the parameter values. Thus, to derive this loss function, we start by considering the entropy in these two random variables *a priori*. That is:

$$\begin{aligned} H(\mathbf{Z}, \boldsymbol{\theta}|\boldsymbol{\xi}) &= \int_{\mathbf{z}} \int_{\boldsymbol{\theta}} p(\mathbf{z}, \boldsymbol{\theta}|\boldsymbol{\xi}) \log p(\mathbf{z}, \boldsymbol{\theta}|\boldsymbol{\xi}) d\mathbf{z} d\boldsymbol{\theta}, \text{ and} \\ H(\mathbf{Z}, \boldsymbol{\theta}|\boldsymbol{\xi}) &= \sum_{\mathbf{z}} \int_{\boldsymbol{\theta}} p(\mathbf{z}, \boldsymbol{\theta}|\boldsymbol{\xi}) \log p(\mathbf{z}, \boldsymbol{\theta}|\boldsymbol{\xi}) d\boldsymbol{\theta}, \end{aligned}$$

for cases where  $\mathbf{Z}$  is a continuous and discrete outcome, respectively.

Following this, we define the loss function in terms of the change in entropy about the predicted outcome and the parameters upon observing data  $\mathbf{y}$  at design  $\mathbf{d}$  as follows:

$$\lambda_D(\mathbf{d}, \mathbf{y}) = H(\mathbf{Z}, \boldsymbol{\theta} | \mathbf{y}, \mathbf{d}, \boldsymbol{\xi}) - H(\mathbf{Z}, \boldsymbol{\theta} | \boldsymbol{\xi}). \quad (6)$$

Using the chain rule of entropy, it is straightforward to show that the joint entropy of the predicted outcome and the parameters is equal to the conditional entropy of the predicted outcome given the parameters plus the entropy of the parameters. That is:

$$H(\mathbf{Z}, \boldsymbol{\theta} | \mathbf{y}, \mathbf{d}, \boldsymbol{\xi}) = H(\mathbf{Z} | \boldsymbol{\theta}, \mathbf{y}, \mathbf{d}, \boldsymbol{\xi}) + H(\boldsymbol{\theta} | \mathbf{y}, \mathbf{d}), \text{ and } H(\mathbf{Z}, \boldsymbol{\theta} | \boldsymbol{\xi}) = H(\mathbf{Z} | \boldsymbol{\theta}, \boldsymbol{\xi}) + H(\boldsymbol{\theta}). \quad (7)$$

Then, by substituting the above expressions in Equation (6), the loss function  $\lambda_D(\mathbf{d}, \mathbf{y})$  can be expressed as follows:

$$\begin{aligned} \lambda_D(\mathbf{d}, \mathbf{y}) &= H(\mathbf{Z}, \boldsymbol{\theta} | \mathbf{y}, \mathbf{d}, \boldsymbol{\xi}) - H(\mathbf{Z}, \boldsymbol{\theta} | \boldsymbol{\xi}) \\ &= \{H(\mathbf{Z} | \boldsymbol{\theta}, \mathbf{y}, \mathbf{d}, \boldsymbol{\xi}) + H(\boldsymbol{\theta} | \mathbf{y}, \mathbf{d})\} - \{H(\mathbf{Z} | \boldsymbol{\theta}, \boldsymbol{\xi}) + H(\boldsymbol{\theta})\} \\ &= \{H(\mathbf{Z} | \boldsymbol{\theta}, \mathbf{y}, \mathbf{d}, \boldsymbol{\xi}) - H(\mathbf{Z} | \boldsymbol{\theta}, \boldsymbol{\xi})\} + \{H(\boldsymbol{\theta} | \mathbf{y}, \mathbf{d}) - H(\boldsymbol{\theta})\} \\ &= \lambda_P(\mathbf{d}, \mathbf{y}) + \lambda_E(\mathbf{d}, \mathbf{y}). \end{aligned} \quad (8)$$

As shown in Equation (8), the loss function  $\lambda_D(\mathbf{y}, \mathbf{d})$  can be expressed as a sum of two loss functions in which the first ( $\lambda_P(\mathbf{y}, \mathbf{d})$ ) quantifies the change in entropy about the predicted outcome given the parameters  $\boldsymbol{\theta}$  while the second ( $\lambda_E(\mathbf{y}, \mathbf{d})$ ) quantifies the change in entropy about the parameter values. Thus, the loss function  $\lambda_D(\mathbf{y}, \mathbf{d})$  is termed as a dual-purpose loss function for parameter estimation and prediction.

Such an expression was considered by [Sebastiani and Wynn \(2000\)](#) for a special class of models where data are assumed to be independent. For such models, it was shown that minimising the above expression is equivalent to minimising  $\lambda_E(\mathbf{d}, \mathbf{y})$  i.e. just focusing on estimation. This can be readily observed, for example, by noting that the entropy of a prediction conditional on a value for the parameter is constant for a regression model with additive, independent and identically distributed errors. This feature was exploited by [Sebastiani and Wynn \(2000\)](#) who proposed *maximum entropy sampling*, an efficient approach for selecting locations to minimise parameter uncertainty. However, for geostatistical models, the errors are not independent or identically distributed, and hence minimising the above loss function is not equivalent to minimising the expected loss associated with the parameters (only). Thus, our work extends research that was previously limited to a special class of models.

For parameter estimation, the loss function  $\lambda_E(\mathbf{y}, \mathbf{d})$  is equivalent to the Kullback-Leibler divergence (KLD) between the prior and the posterior distributions of parameters ([Kullback and Leibler, 1951](#)), and can be expressed as follows:

$$\lambda_E(\mathbf{d}, \mathbf{y}) = - \int_{\boldsymbol{\theta}} p(\boldsymbol{\theta} | \mathbf{y}, \mathbf{d}) \log \left( \frac{p(\boldsymbol{\theta} | \mathbf{y}, \mathbf{d})}{p(\boldsymbol{\theta})} \right) d\boldsymbol{\theta}. \quad (9)$$



When evaluating the loss function  $\lambda_P(\mathbf{y}, \mathbf{d})$  for design selection, the term  $H(\mathbf{Z}|\boldsymbol{\theta}, \boldsymbol{\xi})$  is independent of the design  $\mathbf{d}$ . As such, for simplicity, we consider  $H(\mathbf{Z}|\boldsymbol{\theta}, \mathbf{y}, \mathbf{d}, \boldsymbol{\xi})$  as our loss function for prediction given the parameters as follows:

$$\begin{aligned}\lambda_P(\mathbf{d}, \mathbf{y}) &= H(\mathbf{Z}|\boldsymbol{\theta}, \mathbf{y}, \mathbf{d}, \boldsymbol{\xi}) \\ &= - \int_{\boldsymbol{\theta}} p(\boldsymbol{\theta}|\mathbf{y}, \mathbf{d}) \int_{\mathbf{z}} p(\mathbf{z}|\boldsymbol{\theta}, \mathbf{y}, \mathbf{d}, \boldsymbol{\xi}) \log p(\mathbf{z}|\boldsymbol{\theta}, \mathbf{y}, \mathbf{d}, \boldsymbol{\xi}) d\mathbf{z} d\boldsymbol{\theta}.\end{aligned}\quad (10)$$

When a bivariate mixed outcome (i.e. one outcome is continuous and the other is discrete) is observed ( $\mathbf{y} = (y_1, y_2)$  and  $\mathbf{z} = (z_1, z_2)$ ), the above loss function can be expressed as follows:

$$\lambda_P(\mathbf{d}, \mathbf{y}) = - \int_{\boldsymbol{\theta}} p(\boldsymbol{\theta}|\mathbf{y}, \mathbf{d}) \sum_{z_2} \int_{z_1} p(\mathbf{z}|\boldsymbol{\theta}, \mathbf{y}, \mathbf{d}, \boldsymbol{\xi}) \log p(\mathbf{z}|\boldsymbol{\theta}, \mathbf{y}, \mathbf{d}, \boldsymbol{\xi}) dz_1 d\boldsymbol{\theta}.\quad (11)$$

## 4 Efficient approximations to loss functions

Evaluating the MC approximation to the expected loss in Equation (11) requires approximating or sampling from a large number of posterior distributions. Unfortunately, this renders algorithms like Markov chain Monte Carlo computationally infeasible to use in locating designs. In this section, we describe computationally efficient methods for approximating the posterior distribution. We then show how this is used in approximating the above loss functions.

### 4.1 Approximating the posterior distribution

To efficiently evaluate the MC approximation to the expected loss function in Equation (11), fast methods for approximate inference are required. For this purpose, we consider the Laplace approximation to the posterior distribution, see [Long et al. \(2013\)](#); [Overstall, McGree and Drovandi \(2018\)](#). For this, we assume, approximately, that:

$$(\boldsymbol{\theta}|\mathbf{y}, \mathbf{d}) \sim MVN(\boldsymbol{\theta}^*, \mathbf{A}(\boldsymbol{\theta}^*)^{-1}),$$

where  $\boldsymbol{\theta}^* = \arg \max_{\boldsymbol{\theta}} \{\log(p(\mathbf{y}|\mathbf{d}, \boldsymbol{\theta})) + \log(p(\boldsymbol{\theta}))\}$  and  $\mathbf{A}(\boldsymbol{\theta}^*)$  is the negative Hessian matrix:

$$\mathbf{A}(\boldsymbol{\theta}^*) = \frac{-\partial^2 \{ \log(p(\mathbf{y}|\mathbf{d}, \boldsymbol{\theta})) + \log(p(\boldsymbol{\theta})) \}}{\partial \boldsymbol{\theta} \partial \boldsymbol{\theta}'} \Big|_{\boldsymbol{\theta}=\boldsymbol{\theta}^*}.$$

In our spatial model, the linear predictor contains random effects, and these need to be integrated out in order to evaluate the likelihood. That is:



$$p(\mathbf{y}|\mathbf{d}, \boldsymbol{\theta}) = \int_{\mathbf{s}_1} \cdots \int_{\mathbf{s}_2} \cdots \int \prod_{i=1}^n \prod_{j=1}^{n_i} \left[ (f_{Y_1|s_{1i}}(y_{1ij})) (c_{1ij} - c_{1ij}^*) \right] p(\mathbf{s}_1|\boldsymbol{\gamma}_1) \times \\ p(\mathbf{s}_2|\boldsymbol{\gamma}_2) ds_{11} \dots ds_{1n} ds_{21} \dots ds_{2n}.$$

Unfortunately, given the form of our model, there will typically be no closed-form solution to the above integral, and therefore the likelihood. To handle this, we again employ MC integration to approximate this integral by simulating random effects as follows  $s_{1ib} \sim p(s_{1i}|\boldsymbol{\gamma}_1)$ ,  $ps_{2ib} \sim (s_{2i}|\boldsymbol{\gamma}_2)$  for  $i = 1, 2, \dots, n$  and  $b = 1, 2, \dots, B$ . Then, the likelihood can be approximated as follows:

$$p(\mathbf{y}|\mathbf{d}, \boldsymbol{\theta}) \approx \frac{1}{B} \sum_{b=1}^B \prod_{i=1}^n \prod_{j=1}^{n_i} p(y_{ij}|d_i, \boldsymbol{\theta}, s_{1ib}, s_{2ib}). \quad (12)$$

It is this approximation to the likelihood that is used to form a Laplace approximation to the posterior distribution (as shown above).

## 4.2 Approximating the loss function

When both the prior and posterior distributions follow multivariate Normal distributions with mean vectors  $(\boldsymbol{\mu}_0, \boldsymbol{\mu}_1)$  and covariance matrices  $(\boldsymbol{\Sigma}_0, \boldsymbol{\Sigma}_1)$ , respectively, the loss function  $\lambda_E(\mathbf{y}, \mathbf{d})$  can be evaluated as follows:

$$\tilde{\lambda}_E(\mathbf{d}, \mathbf{y}) = -\frac{1}{2} \left( \text{tr}(\boldsymbol{\Sigma}_0^{-1} \boldsymbol{\Sigma}_1) + (\boldsymbol{\mu}_1 - \boldsymbol{\mu}_0)^T \boldsymbol{\Sigma}_0^{-1} (\boldsymbol{\mu}_1 - \boldsymbol{\mu}_0) - k + \log \left( \frac{\det \boldsymbol{\Sigma}_0}{\det \boldsymbol{\Sigma}_1} \right) \right), \quad (13)$$

where  $k$  is the dimension of the two multivariate Normal distributions.

In terms of approximating  $\hat{\lambda}_P(\mathbf{d}, \mathbf{y})$ , this proves to be a little more complicated as summations need to be taken across simulated values of  $\boldsymbol{\theta}$ ,  $\mathbf{y}$  and  $\mathbf{z}$ . That is:

$$\hat{\lambda}_P(\mathbf{d}, \mathbf{y}) = -\frac{1}{K} \sum_{k=1}^K \frac{1}{R} \sum_{r=1}^R \left[ \log \left( \frac{1}{B} \sum_{b=1}^B p(\mathbf{z}_r | \mathbf{s}_b, \boldsymbol{\theta}_k, \mathbf{y}, \mathbf{d}, \mathbf{x}) \right) \right], \quad (14)$$

where  $\boldsymbol{\theta}_k \sim p(\boldsymbol{\theta}|\mathbf{y}, \mathbf{d})$ ,  $\mathbf{s}_b \sim p(\mathbf{s}|\boldsymbol{\theta}, \mathbf{y}, \mathbf{d})$  and  $\mathbf{z}_r \sim p(\mathbf{z}|\mathbf{s}, \boldsymbol{\theta}, \mathbf{y}, \mathbf{d}, \boldsymbol{\xi})$ .

In using this approach, in order to precisely estimate this loss function, a sufficiently large number of samples should be taken from the posterior distributions of the parameters, random effects, and the posterior predictive distribution (i.e. all  $B$ ,  $K$  and  $R$  should be sufficiently large). Thus, evaluating this loss function is hugely expensive computationally. Indeed, if each integral requires  $N$  MC samples, the computation time is of order  $N^3$  ( $\mathcal{O}(N^3)$ ). Unfortunately, this renders such an approach computationally infeasible for use in locating designs (even when adopting a Laplace approximation to the posterior distribution). To overcome this, we consider forming a Normal approximation to the joint distribution of simulated data and the parameters

$(\mathbf{z}, \boldsymbol{\theta})$ , as the entropy for a Normal distribution has a closed form. We propose forming this approximation via moment matching. That is, in the two examples considered in this paper, a bivariate mixed outcome is observed where a Normal response ( $Y_1$ ) and a Poisson response ( $Y_2$ ) are considered. Given the mean value for the Poisson response is reasonably large, the joint distribution of  $Y_1$  and  $Y_2$  given  $\mathbf{d}$  and  $\boldsymbol{\xi}$  can be approximated by a bivariate Normal distribution. Given this, the entropy of bivariate Normal response was considered to approximate the loss function given in Equation (11), and therefore the first term of the total loss function given in Equation (8) is approximated as follows:

$$\tilde{\lambda}_P(\mathbf{d}, \mathbf{y}) = \frac{1}{2} \sum_{\boldsymbol{\xi}_t \in \boldsymbol{\xi}} \log \det(2\pi e \hat{\boldsymbol{\Sigma}}_{\boldsymbol{\xi}_t}), \quad (15)$$

where  $\log e = 1$  and  $\hat{\boldsymbol{\Sigma}}_{\boldsymbol{\xi}_t}$  is the approximated variance-covariance matrix of the bivariate Normal distribution at location  $\boldsymbol{\xi}_t$ . Here,  $\hat{\boldsymbol{\Sigma}}_{\boldsymbol{\xi}_t}$  was approximated by taking a sufficiently large sample from the posterior predictive distribution  $p(\mathbf{z}|\mathbf{s}, \boldsymbol{\theta}, \mathbf{y}, \mathbf{d}, \boldsymbol{\xi}_t)$ . This approximation has complexity of order  $N$  i.e.  $\mathcal{O}(N)$ , making it substantially more efficient to compute than the approximation in Equation (14). We explore the accuracy of this approximation in Section 5.

As the second term of the dual-purpose loss function in Equation (8) can be approximated by using the KLD formula given in Equation (13), the dual-purpose loss function can be approximated as follows:

$$\tilde{\lambda}_D(\mathbf{d}, \mathbf{y}) = \tilde{\lambda}_P(\mathbf{d}, \mathbf{y}) + \tilde{\lambda}_E(\mathbf{d}, \mathbf{y}). \quad (16)$$

### 4.3 Design algorithm

With the use of the Laplace approximation to the posterior distribution and the above approximation to the expected loss, we propose Algorithm 1 to derive optimal designs for spatially dependent bivariate outcomes described by Copula models.

---

**Algorithm 1** Approximating the expected loss function for the location of geostatistical designs

---

- 1: Initialise the prior information  $p(\boldsymbol{\theta})$  and the prediction region  $\mathcal{A}$ .
  - 2: **for**  $q = 1$  to  $Q$  **do**
  - 3:   Draw  $\boldsymbol{\theta}_q$  from prior  $p(\boldsymbol{\theta})$
  - 4:   Simulate  $\mathbf{s}_q$  from the random effects distribution  $\mathbf{s}_q \sim p(\mathbf{s}|\boldsymbol{\theta}_q)$
  - 5:   Simulate data  $\mathbf{y}_q$  at the design  $\mathbf{d}$  from the assumed Copula model  $\mathbf{y}_q \sim p(\mathbf{y}|\mathbf{s}_q, \boldsymbol{\theta}_q, \mathbf{d})$
  - 6:   Find Laplace approximation  $\boldsymbol{\theta}_q^* = \arg \max_{\boldsymbol{\theta}} \{\log(p(\mathbf{y}_q|\boldsymbol{\theta}, \mathbf{d})) + \log(p(\boldsymbol{\theta}))\}$  such that  
the posterior distribution can be approximated by  $MVN(\boldsymbol{\theta}_q^*, \mathbf{A}_q^{-1})$ , where  
 $\mathbf{A}_q$  is the Hessian matrix defined as:
$$\mathbf{A}_q = \frac{-\partial^2 \{ \log(p(\mathbf{y}_q|\boldsymbol{\theta}, \mathbf{d})) + \log(p(\boldsymbol{\theta})) \}}{\partial \boldsymbol{\theta} \partial \boldsymbol{\theta}'} \Big|_{\boldsymbol{\theta}=\boldsymbol{\theta}^*}.$$
  - 7:   Approximate the information loss  $\tilde{\lambda}_D(\mathbf{d}, \mathbf{y}_q)$  using in Equation (16).
  - 8: **end for**
  - 9: Approximate the expected loss  $\hat{L}(\mathbf{d}) = \frac{1}{Q} \sum_{q=1}^Q \tilde{\lambda}_D(\mathbf{d}, \mathbf{y}_q)$ .
  - 10: Find optimal design  $\mathbf{d}^* = \arg \min_{\mathbf{d} \in \mathcal{D}} \hat{L}(\mathbf{d})$ .
- 

Implementing this algorithm requires defining a model for analysis, the prior information about the parameters and the prediction region (line 1). Once defined, at each iteration, a single particle  $\boldsymbol{\theta}_q$  is drawn from the prior distribution (line 3). Then, for a given  $\boldsymbol{\theta}_q$ , a random effect  $\mathbf{s}_q$  is simulated (line 4). Next, data  $\mathbf{y}_q$  are simulated from the assumed Copula model (line 5). The posterior distribution of the parameter is then found via the Laplace approximation (line 6). For this, the random effects need to be integrated out when evaluating the likelihood for Laplace approximation (see Equation (12)). When the dual-purpose loss function is considered for design selection,  $\lambda_D(\mathbf{d}, \mathbf{y}_q)$  in line 7 of Algorithm 1 can be approximated via Equation (16). When finding optimal estimation designs with Normal prior distributions, the loss function  $\lambda_E(\mathbf{d}, \mathbf{y}_q)$  can be found analytically (see Equation (13)). Then, once  $Q$  iterations have been completed, the MC approximation to the expected loss is evaluated in line 9. To find the optimal set of locations, a suitable optimisation algorithm is implemented to minimise the approximate expected loss function (line 10).

## 5 Case studies

Two examples are considered to demonstrate the performance of Algorithm 1 and the dual-purpose loss function derived in Section 3. In both examples, bivariate mixed spatial outcomes are observed. As such, we first model the individual spatial outcomes by using GLSMs, and then combine these via the Clayton Copula model as described in Section 2.2.

In Example 1, we simulate data within a unit square with a squared exponential covariance function under parameter uncertainty. As it is unknown whether designs vary depending upon the strength of spatial dependence, three different settings (weak, moderate and strong) are considered. In Example 2, we apply the proposed approach to re-design the Queensland air quality monitoring network based on two measures of air pollution.

In both of these examples, we consider the case where a practitioner needs to select the most appropriate set of locations to collect data from either an infinite or finite set of locations. To explore this, we evaluated the effectiveness of selecting dual-purpose designs compared to designs that only address a single aim. For this, we first obtained prediction only and estimation only designs using the loss functions given in Equation (5) and Equation (9), respectively. Then, the dual-purpose designs were evaluated against these single-purpose designs to determine efficiency. As Example 1 considers a continuous design space, the approximate coordinate exchange (ACE) algorithm (Overstall and Woods, 2017) was used to find optimal designs. Here, default settings as detailed in Overstall, Woods and Adamou (2018) were used. As Example 2 was undertaken across a restricted design space with only a fixed number of locations being available, the standard coordinate exchange algorithm (Meyer and Nachtsheim, 1995) was used to obtain optimal designs. All simulations were run using R 3.5.2, and R code to reproduce the results in this paper is available via the following GitHub repository, [https://github.com/SenarathneSGJ/Model-based\\_geostatistical\\_design](https://github.com/SenarathneSGJ/Model-based_geostatistical_design).

### 5.1 Example 1: Exploring dual-purpose design for spatial processes

In this example, we consider collecting bivariate outcomes across a spatial process. Here, response 1 ( $Y_1$ ) was assumed to follow a Normal distribution given the random effects  $s_1$  as follows:

$$Y_1|s_1 \sim N(\mu_1, \sigma_1^2) \quad \text{and} \quad \mu_1 = \beta_{10} + \beta_{11}X_1 + \beta_{12}X_2 + s_1, \quad (17)$$

where  $\{\beta_{10}, \beta_{11}, \beta_{12}\}$  are the model parameters,  $X_1$  and  $X_2$  are the two covariates in the model and  $\sigma_1^2$  is the residual variance of the continuous outcome  $Y_1$ . The random effects  $s_1$  were assumed to follow a multivariate normal distribution with mean  $\mathbf{0}$  and covariance matrix  $\Sigma_1$ , where the elements of  $\Sigma_1$  were obtained via a squared exponential covariance function with parameters  $\{\gamma_{10}, \gamma_{11}, \gamma_{12}\}$  as described in Section 2.

Response 2 ( $Y_2$ ) was assumed to follow a Poisson distribution given the random effects  $s_2$  as follows:

$$Y_2|s_2 \sim \text{Pois}(\exp(\mu_2)) \quad \text{and} \quad \mu_2 = \beta_{20} + \beta_{21}X_1 + \beta_{22}X_2 + s_2, \quad (18)$$

where  $\{\beta_{20}, \beta_{21}, \beta_{22}\}$  are the model parameters, and  $X_1, X_2$  are two covariates of the model. Again, the random effects  $s_2$  were assumed to follow a multivariate normal distribution with mean  $\mathbf{0}$  and covariance matrix  $\Sigma_2$ . The elements of the covariance matrix  $\Sigma_2$  were obtained from a squared exponential covariance function with parameters  $\{\gamma_{20}, \gamma_{21}, \gamma_{22}\}$ .

Next, the model for the multiple responses  $Y_1$  and  $Y_2$  was obtained using the Clayton Copula function as detailed in the previous section. It was assumed that accurate predictions were required at 25 locations ( $\xi$ ) defined as follows:

$$\xi_{vw} = (0.25v, 0.25w) \text{ for } v, w = 0, 1, \dots, 4.$$

To investigate the performance of our design algorithm and the dual-purpose loss function for obtaining the optimal design under various spatial conditions, three design scenarios were

considered. These design scenarios differ in terms of the strength of the spatial covariance, constructed via three different values for the prior mean of the spatial range parameter as given in Table 1.

Table 1: Strength of the covariance in three scenarios

Scenario	Strength of dependence	Prior mean of range parameter ( $a$ )
1	Weak	0.2
2	Moderate	0.5
3	Strong	0.8

The prior distributions of the remaining parameters were same across all the scenarios. For all the model and covariance parameters Normal priors were considered as defined in Table 2. Further, we assumed that there is a positive dependence between the two responses, and therefore, a Normal prior was considered for the parameter  $\text{logit}(\tau)$ , which we also estimated within our framework.

Table 2: Prior distributions for all parameters

Parameter	Prior distribution	Parameter	Prior distribution
$\beta_{10}$	$N(5, 4)$	$\beta_{20}$	$N(3.8, 0.125)$
$\beta_{11}$	$N(-2.8, 4)$	$\beta_{21}$	$N(-1.5, 0.125)$
$\beta_{12}$	$N(8, 4)$	$\beta_{22}$	$N(-1.2, 0.125)$
$\log(\sigma_1)$	$N(\log(1.2), 0.25)$	$\log(\gamma_{21}/\gamma_{22})$	$N(\log(0.6/a), 0.125)$
$\log(\gamma_{11}/\gamma_{12})$	$N(\log(0.7/a), 0.25)$	$\log(\gamma_{22})$	$N(\log(a), 0.125)$
$\log(\gamma_{12})$	$N(\log(a), 0.25)$	$\text{logit}(\tau)$	$N(0.85, 0.25)$

\*The parameter  $a \in \{0.2, 0.5, 0.8\}$ .

For this example, we set  $\gamma_{10} = 0.001$  and  $\gamma_{20} = 0.001$ . That is, the impact of the nugget effect on spatial covariance is negligible when compared to the spatial range and partial sill parameters.

**Results:** We first explore the accuracy of the proposed approximation to the loss function  $\lambda_P(\mathbf{d}, \mathbf{y})$  in Equation (15). To do this, we evaluated  $\tilde{\lambda}_P(\mathbf{d}, \mathbf{y})$  and  $\hat{\lambda}_P(\mathbf{d}, \mathbf{y})$  for 100 randomly generated designs under moderate spatial dependence. The results of this are shown in Figure 1 where a clear but noisy relationship between the two loss functions can be observed. Despite the noise, there is generally agreement between the two approximations, particularly in terms of designs that minimise each loss function. Similar results were also observed under weak and strong spatial dependence. As such, we propose that our approximation can be used to selection designs for this example.

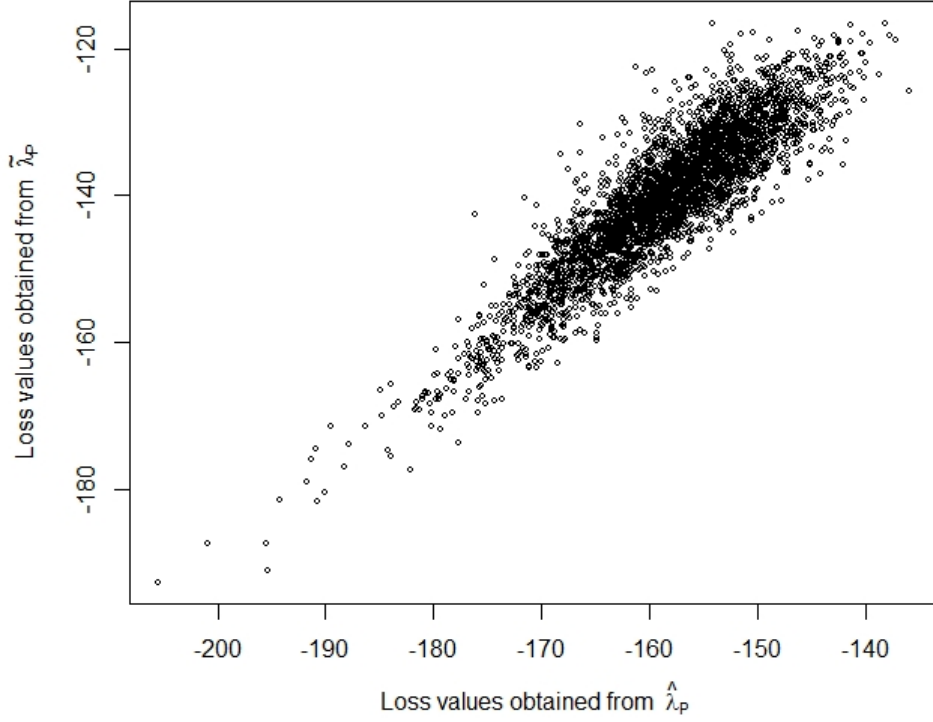


Figure 1: The relationship between the loss values obtained from  $\hat{\lambda}_P(\mathbf{d}, \mathbf{y})$  and  $\tilde{\lambda}_P(\mathbf{d}, \mathbf{y})$  for 100 randomly generated designs under moderate spatial dependence from Example 1

Figures 2 and 3 compare the optimal designs selected under the three scenarios with 5 and 10 locations, respectively. As can be seen, when there is moderate or strong spatial covariance, the designs selected under the three loss functions have different spatial configurations. When spatial covariance is weak, spatial configurations of the dual-purpose designs appear to be similar to the prediction designs.

Once the optimal designs had been found for each scenario, they were evaluated for the goals of parameter estimation and spatial prediction. For this evaluation, 100 independent simulations were used. In each simulation, for a given optimal design, the expected values of the loss functions  $\lambda_E(\mathbf{d}, \mathbf{y})$  and  $\lambda_P(\mathbf{d}, \mathbf{y})$  were estimated using the MC integration as shown in Equation (4). This yielded a distribution of the expected loss values for each optimal design (see Figure 4 and Figure 5). Further, to quantitatively compare designs, a design efficiency was calculated. For this purpose, the average of the 100 expected loss values was used as follows:

$$\text{Eff}(\mathbf{d}, \mathbf{d}_\phi^*) = \frac{\frac{1}{100} \sum_{k=1}^{100} E_{\mathbf{y}_k}[\lambda_\phi(\mathbf{d}, \mathbf{y}_k)]}{\frac{1}{100} \sum_{k=1}^{100} E_{\mathbf{y}_k}[\lambda_\phi(\mathbf{d}_\phi^*, \mathbf{y}_k)]}, \text{ for } \phi \in \{E, P\},$$

where  $\mathbf{d}_E^*$  and  $\mathbf{d}_P^*$  are the optimal designs selected from the loss functions  $\lambda_E(\mathbf{d}, \mathbf{y})$  and  $\lambda_P(\mathbf{d}, \mathbf{y})$ , respectively.

Figure 4 shows the parameter estimation performance of designs selected under each loss function. As expected, the estimation designs have the lowest value of expected loss within each scenario. Of note is the fact that the dual-purpose designs are generally highly efficient when  $n = 10$ , and this efficiency appears to increase with the spatial dependency. The prediction only designs (selected from  $\tilde{\lambda}_P(\mathbf{d}, \mathbf{y})$ ) did not perform well for the goal of parameter estimation,

and this appears to become worse as the strength of spatial dependence increases.

Figure 5 shows the distribution of the expected loss values for different designs when the goal was prediction. As can be seen, the prediction only designs have the lowest expected loss when compared to the other designs. The dual-purpose designs are highly efficient with respect to the prediction (only) designs. Of note, this high efficiency is obtained despite the estimation designs on occasion being relatively inefficient.

Table 3 compares the efficiency of designs found under each experimental goal. These results reflect those seen in the above figures in that the dual-purpose designs are efficient under each objective, and there are occasions when the estimation designs perform relatively poorly for prediction. In contrast, the prediction designs maintain reasonable efficiency for estimation but not to the same extent as the dual-purpose designs.

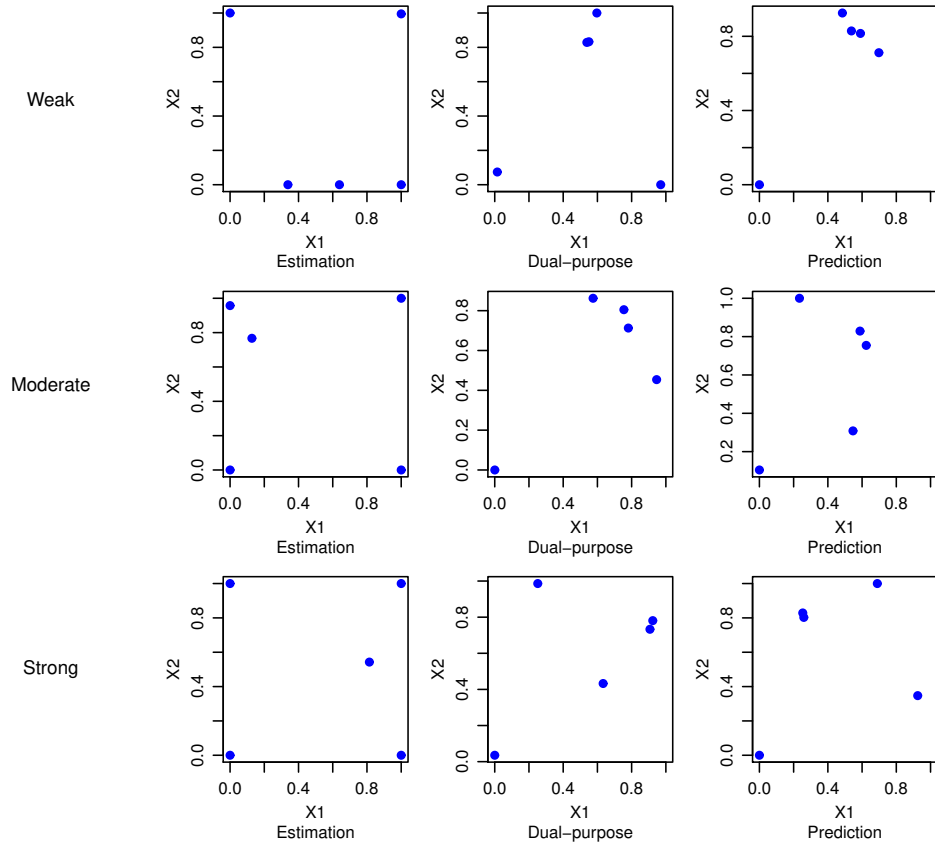


Figure 2: The optimal designs selected from each loss function (n=5)



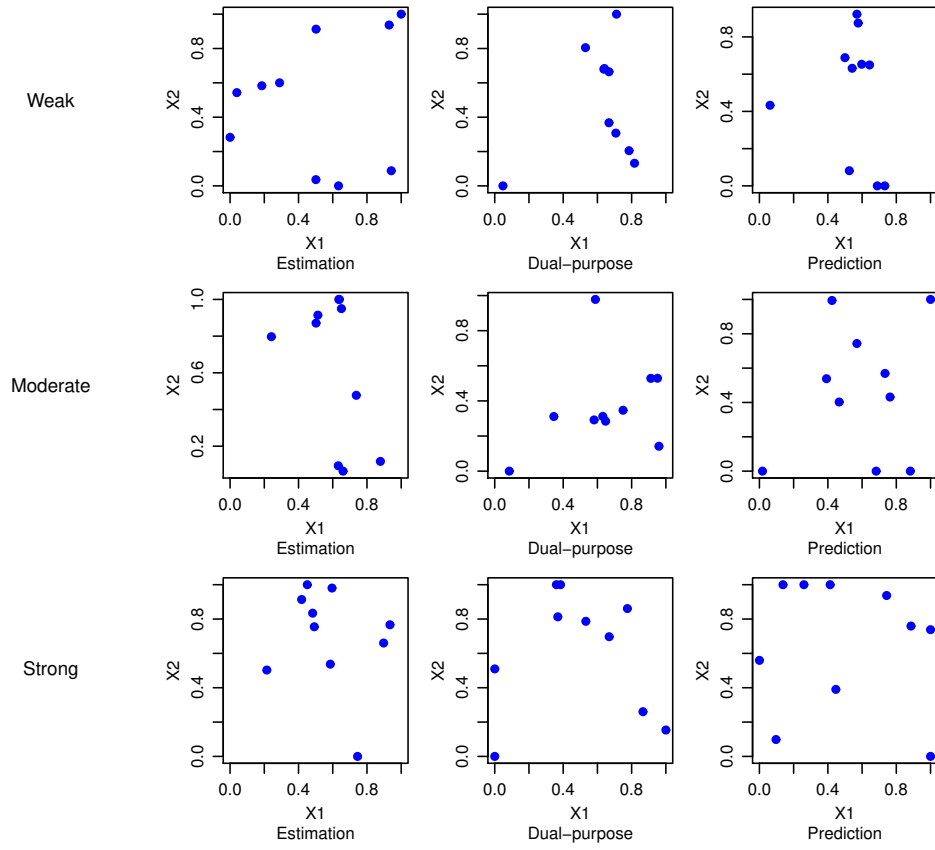


Figure 3: The optimal designs selected from each loss function (n=10)

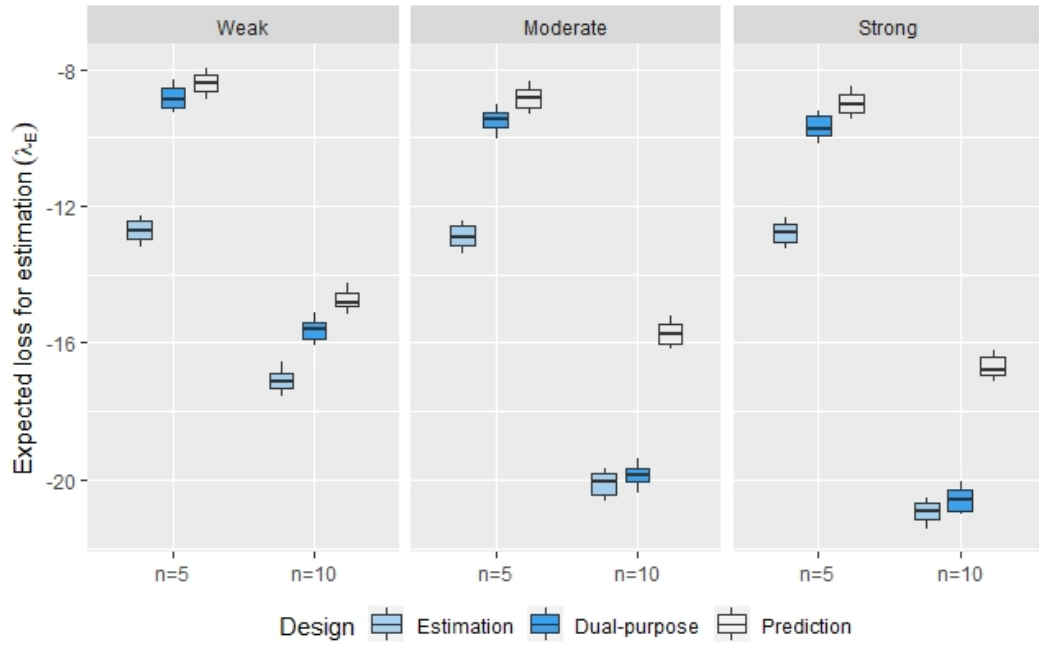


Figure 4: The boxplot of the distribution of the expected values for the loss function that focuses on parameter estimation for different designs over 100 simulations in Example 1

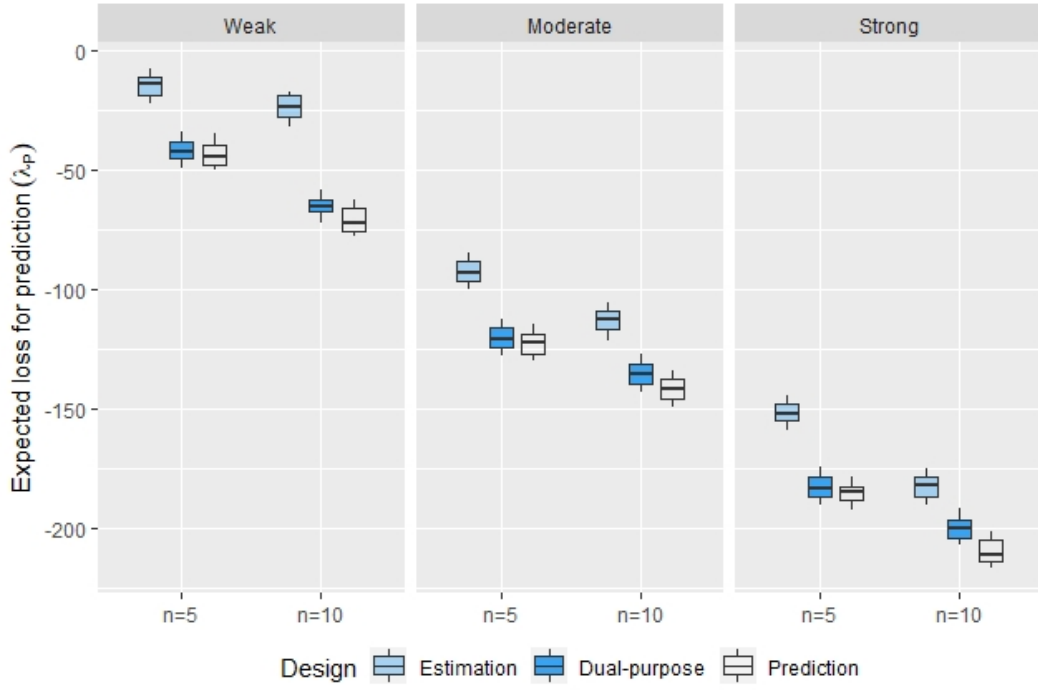


Figure 5: The boxplot of the distribution of the expected values for the loss function that focuses on prediction for different designs over 100 simulations in Example 1

Table 3: Efficiencies of designs selected under each loss function from Example 1

Number of design points	Spatial correlation	Loss function	Estimation efficiency (%)	Prediction efficiency (%)
5	Weak	Estimation	100.00	37.81
		Dual-purpose	70.51	98.45
		Prediction	66.63	100.00
	Moderate	Estimation	100.00	76.02
		Dual-purpose	73.91	98.76
		Prediction	68.90	100.00
	Strong	Estimation	100.00	83.89
		Dual-purpose	75.34	99.93
		Prediction	70.03	100.00
10	Weak	Estimation	100.00	38.80
		Dual-purpose	91.17	93.69
		Prediction	85.90	100.00
	Moderate	Estimation	100.00	78.64
		Dual-purpose	99.24	94.47
		Prediction	78.25	100.00
	Strong	Estimation	100.00	87.30
		Dual-purpose	98.05	95.18
		Prediction	78.98	100.00

## 5.2 Example 2: Designing an air quality monitoring network

Here, we assess the performance of Algorithm 1 and the dual-purpose loss function in finding optimal locations (stations) for an air quality monitoring network based on two pollutants  $NO_2$  and  $PM_{2.5}$ . For this example, the Queensland air quality monitoring network with 22 monitoring stations was considered, where seven stations measured both  $NO_2$  and  $PM_{2.5}$  concentrations. Figure 6 shows the spatial configuration of the sampled and unsampled stations where stations which measure both  $NO_2$  and  $PM_{2.5}$  concentrations are termed as “sampled” locations and the remaining stations are termed as “unsampled” locations.

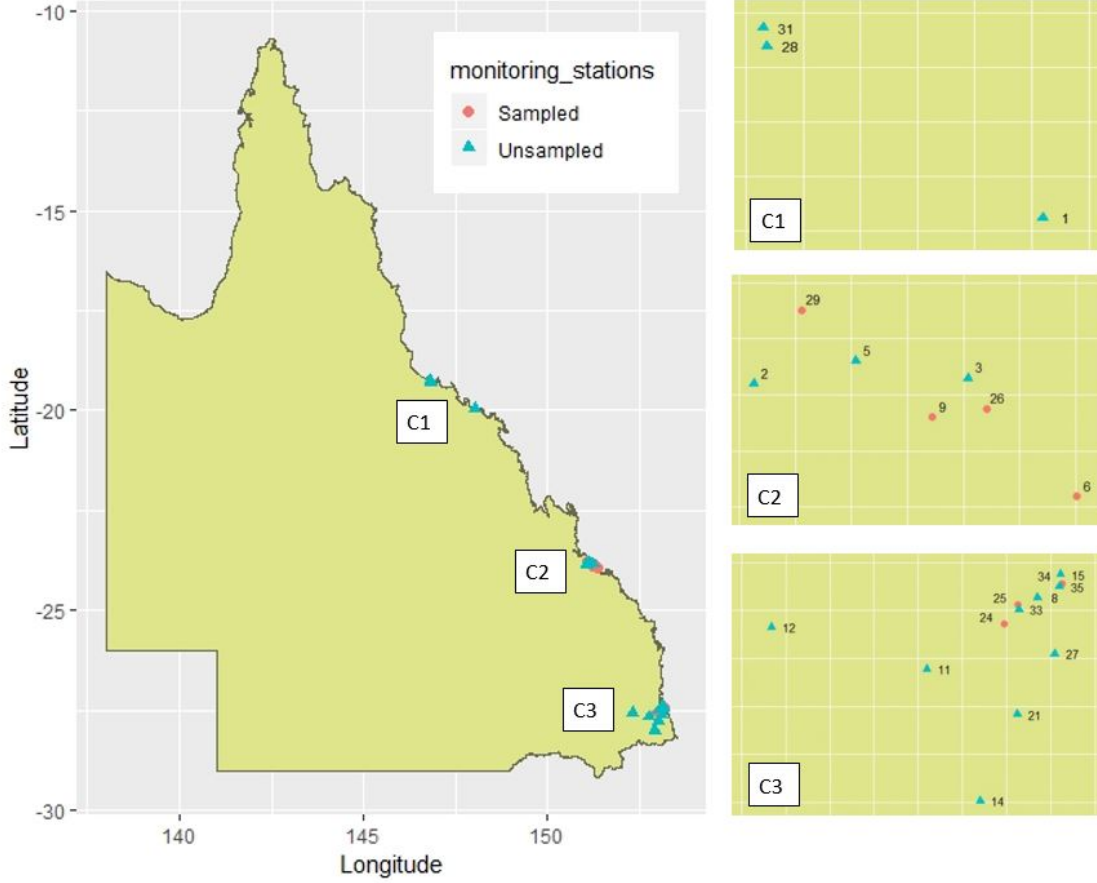


Figure 6: The locations of the selected air quality monitoring stations

For the sampled locations, the annual mean  $NO_2$  concentrations ( $Y_1$ ), the number of days (per annum) which exceed the daily  $PM_{2.5}$  limit of  $10\mu gm^{-3}$  ( $Y_2$ ), and meteorological data from year 2013 to 2016 were collected from the Queensland government website (<https://data.qld.gov.au/dataset>). Then, a GLSM was developed for each response. Similar to Example 1, the response 1 ( $Y_1$ ) was assumed to follow a Normal distribution while responses 2 ( $Y_2$ ) was assumed to follow a Poisson distribution as follows:

$$Y_1|s_1 \sim N(\mu_1, \sigma^2) \quad \text{and} \quad \mu_1 = \beta_{10} + \beta_{11}X_1 + \beta_{12}X_2 + s_1,$$

$$Y_2|s_2 \sim Pois(\exp(\mu_2)) \quad \text{and} \quad \mu_2 = \beta_{20} + \beta_{21}X_1 + \beta_{22}X_3 + s_2,$$

where  $X_1$ ,  $X_2$  and  $X_3$  are the Y-coordinate (in UTM system), annual mean humidity level, and the annual mean wind speed measured at the given location, respectively. Again, the squared

exponential covariance function with parameters  $(\gamma_1, \gamma_2)$  was used to form each variance-covariance matrix to capture the spatial variability in each response.

For this example, we set  $\gamma_{10} = 0.001$  and  $\gamma_{20} = 0.01$ . To find the prior distributions for the remaining parameters, we considered the data collected from the sampled locations over the period from 2013 to 2016. First, for each parameter, vague prior distributions were assumed. Then, the observed data were used to update this prior information, and hence to obtain a posterior distribution. To obtain this posterior distribution, the Laplace approximation discussed in Section 4 was used. It is this posterior distribution that was used for design selection as detailed in Algorithm 1. Here, the purpose of this experiment is to select an optimal set of monitoring stations to collect data so that they can be used to predict the annual  $NO_2$  and  $PM_{2.5}$  concentrations for all the monitoring stations in the network. As such, the optimal design is selected from all available locations across the network (i.e. both sampled and unsampled locations).

**Results:** Similar to the first example, we compared values of loss functions  $\tilde{\lambda}_P(\mathbf{d}, \mathbf{y})$  and  $\hat{\lambda}_P(\mathbf{d}, \mathbf{y})$  for 100 randomly generated designs. Again, similar loss function values were obtained from each approximation, see Figure 7. As such, adopting our approximation to form efficient designs seems reasonable in this example.

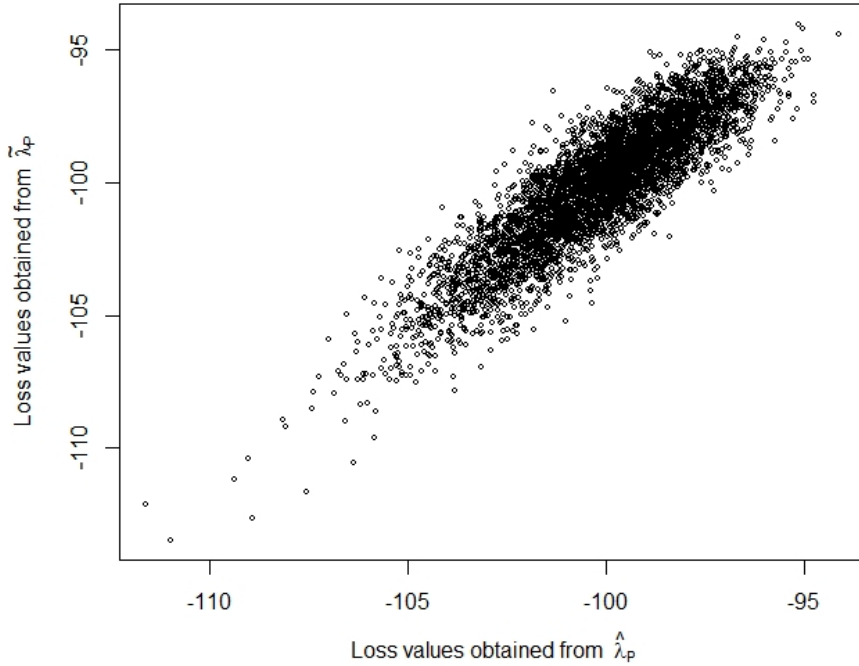


Figure 7: The relationship between the loss values obtained from  $\hat{\lambda}_P(\mathbf{d}, \mathbf{y})$  and  $\tilde{\lambda}_P(\mathbf{d}, \mathbf{y})$  for 100 randomly generated designs from Example 2

In Table 4, we have summarised designs found for different values of  $n$  under each loss function. The numbers shown in this table correspond to the monitoring stations in Figure 6, with the bold numbers representing the sampled locations. Figure 8 shows the locations of the selected monitoring stations under each loss function. It can be seen that the designs selected under each loss function are different but have common stations. Further, when comparing the designs with 5 or 7 design points, it can be seen that the designs points selected from  $\lambda_E(\mathbf{d}, \mathbf{y})$  were spread over the three clusters (C1, C2 and C3) while the majority of design points selected

from  $\lambda_P(\mathbf{d}, \mathbf{y})$  and  $\lambda_D(\mathbf{d}, \mathbf{y})$  were clustered in C3. Since a large number of predicted locations belonged to C3, to minimise the prediction uncertainty, it is reasonable to select more design points from C3 when  $\lambda_P(\mathbf{d}, \mathbf{y})$  and  $\lambda_D(\mathbf{d}, \mathbf{y})$  were responsible for design selection. For the designs with 10 or 15 design points, the prediction only design points were also spread over the three clusters while the majority of dual-purpose design points were clustered around sampled locations in C2 and C3.

After locating the designs under each loss function, parameter estimation and prediction performance was assessed. Similar to Example 1, we considered 100 independent simulations to evaluate the expected loss under each design objective. Figure 9 shows the distribution of values of the expected loss in terms of parameter estimation under different designs. Similar to Example 1, all estimation designs have lower expected loss when compared to other designs. As in the simulated example, the dual-purpose designs appear to be highly efficient in terms of parameter estimation, and this efficiency appears to increase with  $n$ . The results also show that the relative performance of the prediction designs decreases as  $n$  increases. Figure 10 shows the distribution of expected loss values under the prediction loss function for different designs. As can be seen, the designs selected under the dual-purpose loss function perform well compared to the prediction only designs. Further, the relative performance of the estimation designs for prediction appears to decrease with  $n$ .

Table 5 shows the design efficiencies in terms of parameter estimation and prediction. Of note, the dual-purpose designs generally maintain high efficiency under both objectives. For designs found under the other two objectives, there are occasions each perform relatively poorly, highlighted by efficiencies of less than 70%.

Table 4: The optimal monitoring stations selected under each loss function

$n$	Estimation design	Dual-purpose design	Prediction design
5	1,5,15,31, <b>34</b>	8,11,21,27,33	5,11, <b>25</b> ,27,33
7	5,15, <b>24</b> ,27,28,31, <b>34</b>	8,11,14,21,27,33,35	8,11,14,21, <b>24</b> ,27,33
10	2,3, <b>6</b> ,8,11,12,15, <b>25</b> ,27, <b>34</b>	<b>6</b> ,11,12,21, <b>24</b> , <b>25</b> ,27,33, <b>34</b> ,35	1,2,5,8,14, <b>26</b> ,27,28,33,35
15	<b>6</b> ,8, <b>9</b> ,11,12,14,15,21, <b>25</b> , <b>26</b> , <b>29</b> ,31,33, <b>34</b> ,35	1,2,3,5, <b>6</b> ,11,14,15,21, <b>24</b> , <b>25</b> ,27,33, <b>34</b> ,35	5, <b>6</b> ,8, <b>9</b> ,11,12,21, <b>24</b> , <b>25</b> , <b>26</b> , 27,28,31,33, <b>34</b>

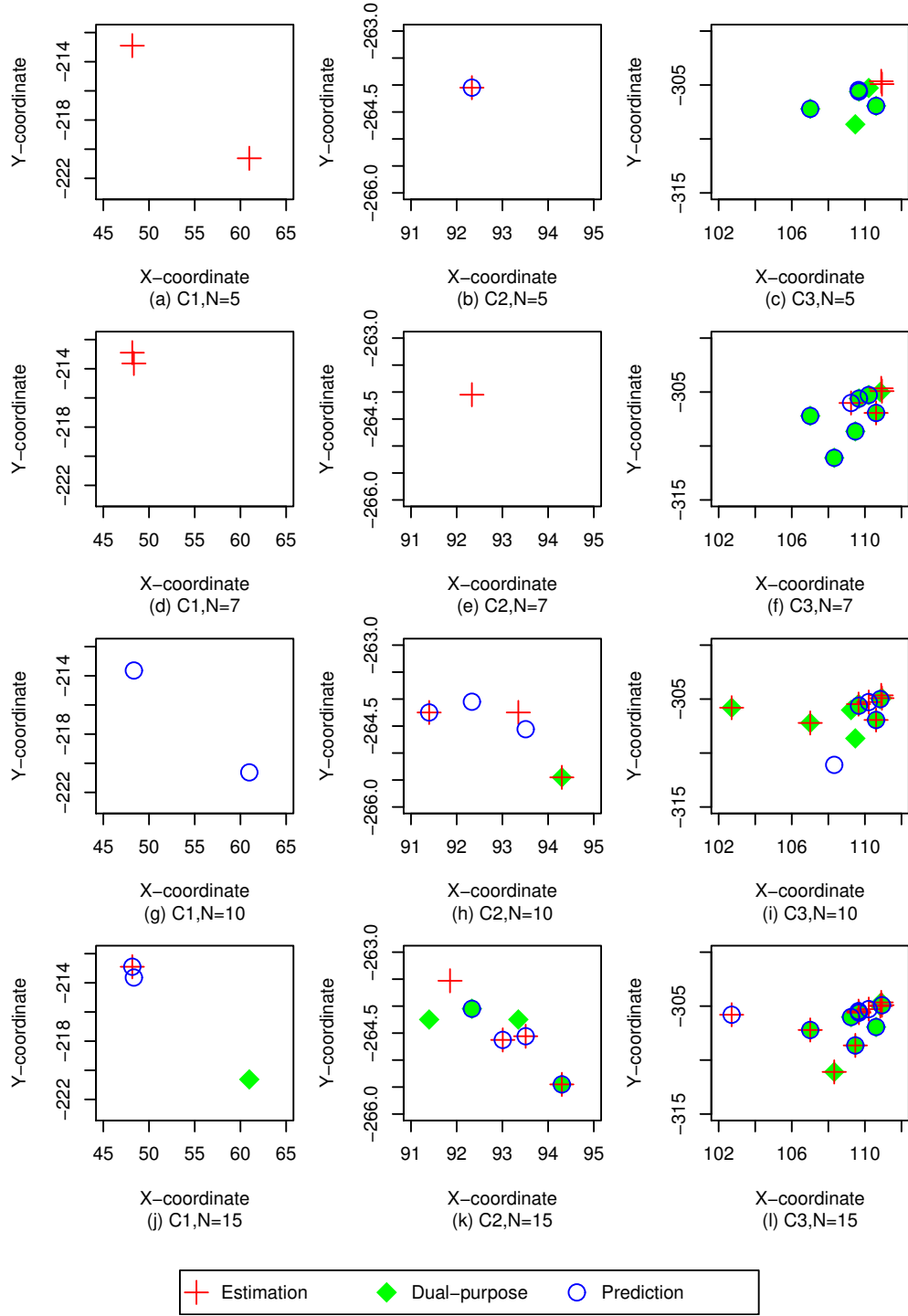


Figure 8: The optimal monitoring stations selected from each loss function

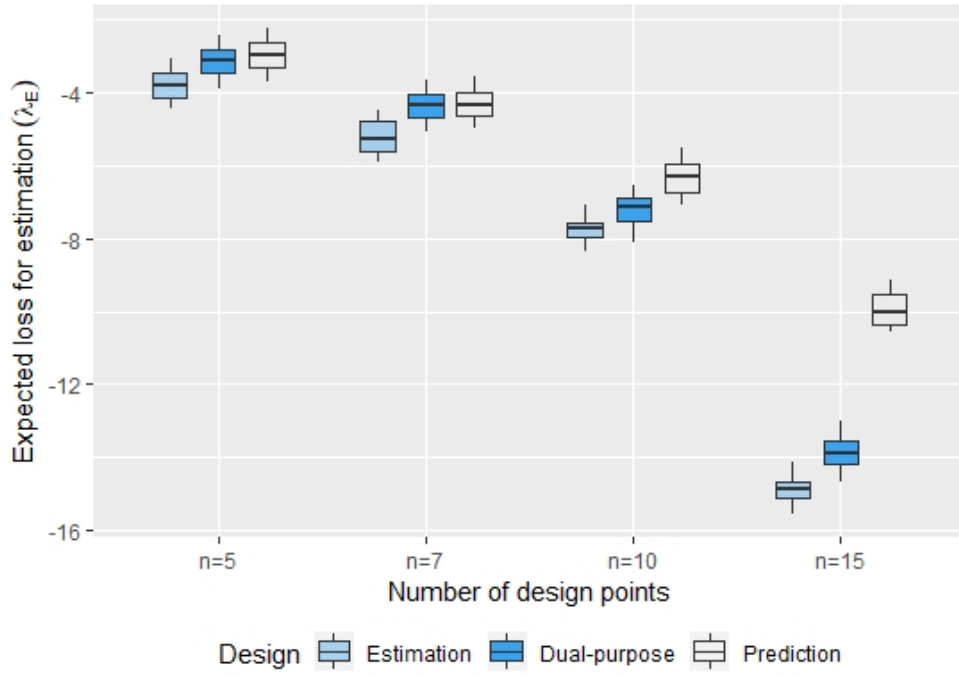


Figure 9: The boxplot of the distribution of the expected values for the loss function that focuses on parameter estimation for different designs over 50 simulations in Example 2

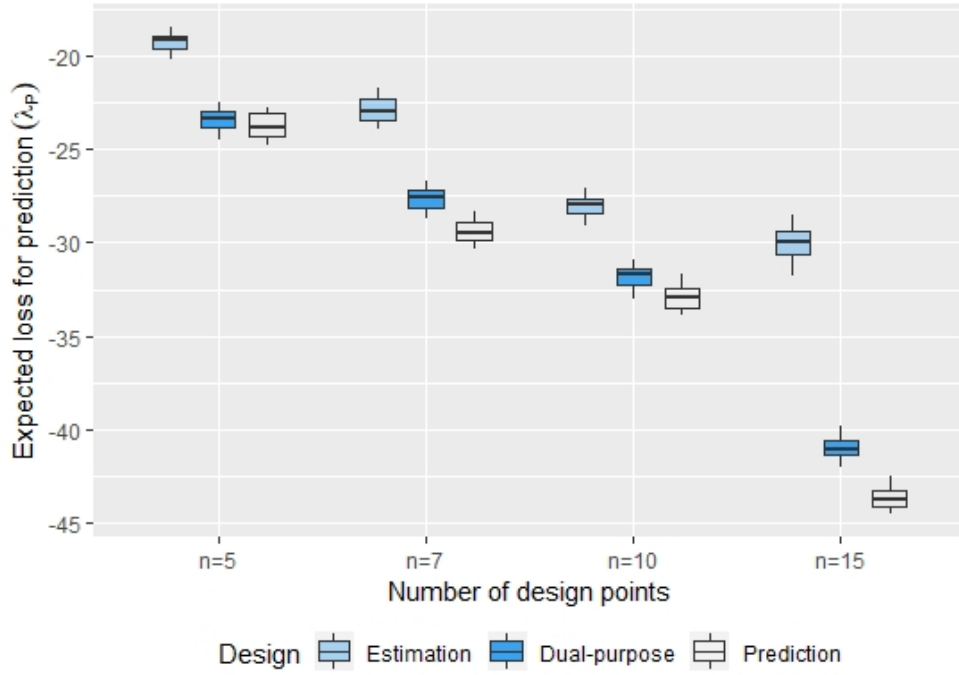


Figure 10: The boxplot of the distribution of the expected values for the loss function that focuses on prediction for different designs over 50 simulations in Example 2



Table 5: Efficiencies of designs selected under each loss function from Example 2

Number of design points	Loss function	Estimation efficiency (%)	Prediction efficiency (%)
5	Estimation	100.00	79.18
	Dual-purpose	82.52	98.38
	Prediction	75.32	100.00
7	Estimation	100.00	77.80
	Dual-purpose	82.71	93.42
	Prediction	81.58	100.00
10	Estimation	100.00	84.60
	Dual-purpose	95.63	97.33
	Prediction	81.50	100.00
15	Estimation	100.00	68.55
	Dual-purpose	91.95	93.46
	Prediction	64.26	100.00

To further investigate future designs for monitoring air quality in Queensland, we re-ran this example by only considering the monitoring stations in C3. Optimal designs with 5 and 7 design points were selected using the three loss functions with the same prior distribution as detailed at the beginning of this example. The selected optimal designs are shown in Figure 11 in the Appendix. Similar to the above results, the dual-purpose designs remain highly efficient for both design objectives (see Table 6). Further, the relative performance of the single purpose designs appear to decrease as  $n$  increases, see Figures 12 and 13.

## 6 Discussion

In this paper, we have developed a Bayesian design approach to minimise uncertainty in spatial processes. The approach is based on the derivation of a dual-purpose loss function which quantifies the uncertainty in a given spatial process. In using this loss function, we extended work which was previously only applicable to a special class of models, and thus facilitating the use of such Bayesian design approaches in geostatistical contexts. In addition, we extended our methodology to handle multiple responses at each location, and this was motivated by what is observed in real-world studies.

In the first example, three design scenarios were considered to test our proposed algorithm and the dual-purpose loss function under various levels of spatial dependence. Overall, the results showed that the dual-purpose designs remained highly efficient under each objective, and this was despite some single objective designs being inefficient under the other objective. Similar results were observed when designing Queensland’s air quality monitoring network based on two air quality measurements  $NO_2$  and  $PM_{2.5}$ . The selection of these two pollutants was motivated by their known adverse effects on human health [Roberts et al. \(2019\)](#); [Huang et al. \(2019\)](#). Despite this, both are only measured at 7 stations across Queensland. Through the use of the new methodologies proposed in this paper, we were able to determine subsets of stations that would yield accurate predictions across the entire network. Thus, adoption of our new methods has real potential to improve air quality monitoring in Queensland. The clustered

nature of the stations (in terms of spatial locations) was accounted for via the range parameter in our covariance function which resulted in the three clusters being independent. Alternative approaches and/or covariance functions to account for this clustering could be considered in the future, and this may have implications in terms of the design.

Despite the theoretical underpinnings of the loss functions developed in this study, the computational complexity of the loss function  $\lambda_P(\mathbf{d}, \mathbf{y})$  is a drawback of this design approach. Indeed, this difficulty led to the development of an efficient approximation based on the joint distribution of the parameters and the data. For the models considered in this paper, this was shown to yield a reasonable approximation. However, such an approach may not be appropriate in general. For example, if bivariate continuous and binary data were observed, it is unlikely that a multivariate normal approximation will be appropriate for estimating the entropy of the distribution of the data. As such, alternative methods are needed, and this is an area we plan to explore into the future.

Another possible extension to this work could include quantifying the uncertainty in different components of the spatial process. This can be achieved by quantifying the uncertainty in the mean model and the covariance function, potentially following the work of [Borth \(1975\)](#); [McGree \(2017\)](#). The proposed loss function could then consider a set of all plausible mean and covariance functions, which is flexible enough to represent the uncertainty in the spatial process ([Pilz et al., 1997](#)). Other areas we hope to pursue into the future include extensions to quantify uncertainty in temporal (and thus, spatio-temporal) processes ([Liu and Vanhatalo, 2019](#)).

## Acknowledgement

SGJS was supported by QUTPRA scholarship from the Queensland University of Technology. Computational resources and services used in this work were provided by the HPC and Research Support Group, Queensland University of Technology, Brisbane, Australia.

## References

- Albert, P. S. and McShane, L. M. (1995), ‘A generalized estimating equations approach for spatially correlated binary data: Applications to the analysis of neuroimaging data’, *Biometrics* **51**(2), 627–638.
- Bárdossy, A. (2006), ‘Copula-based geostatistical models for groundwater quality parameters’, *Water Resources Research* **42**(11).
- Bloom, L. M. and Kentwell, D. J. (1999), A geostatistical analysis of cropped and uncropped soil from the jimperding brook catchment of western australia, *in* J. Gómez-Hernández, A. Soares and R. Froidevaux, eds, ‘geoENV II — Geostatistics for Environmental Applications’, Springer Netherlands, Dordrecht, pp. 369–379.
- Bohorquez, M., Giraldo, R. and Mateu, J. (2017), ‘Multivariate functional random fields: prediction and optimal sampling’, *Stochastic Environmental Research and Risk Assessment* **31**(1), 53–70.
- Borth, D. M. (1975), ‘A total entropy criterion for the dual problem of model discrimination

- and parameter estimation', *Journal of the Royal Statistical Society. Series B (Methodological)* pp. 77–87.
- Bruno, R., Palumbo, V. and Bonduà, S. (2001), Identification of regional variability component by geostatistical analysis of stream sediments, in P. Monestiez, D. Allard and R. Froidevaux, eds, 'geoENV III — Geostatistics for Environmental Applications', Springer Netherlands, Dordrecht, pp. 113–123.
- Castrignanò, A., Buttafuoco, G. and Giasi, C. (2008), Assessment of groundwater salinisation risk using multivariate geostatistics, in A. Soares, M. J. Pereira and R. Dimitrakopoulos, eds, 'geoENV VI – Geostatistics for Environmental Applications: Proceedings of the Sixth European Conference on Geostatistics for Environmental Applications', Springer Netherlands, Dordrecht, pp. 191–202.
- Clayton, D. G. (1978), 'A model for association in bivariate life tables and its application in epidemiological studies of familial tendency in chronic disease incidence', *Biometrika* **65**(1), 141–151.
- Cook, R. D. and Johnson, M. E. (1981), 'A family of distributions for modelling non-elliptically symmetric multivariate data', *Journal of the Royal Statistical Society. Series B (Methodological)* **43**(2), 210–218.
- Cook, R. D. and Wong, W. K. (1994), 'On the equivalence of constrained and compound optimal designs', *Journal of the American Statistical Association* **89**(426), 687–692.
- Diggle, P. J., Ribeiro, P. J. and Christensen, O. F. (2003), An introduction to model-based geostatistics, in J. Møller, ed., 'Spatial Statistics and Computational Methods', Springer New York, pp. 43–86.
- Diggle, P. and Lophaven, S. (2006), 'Bayesian geostatistical design', *Scandinavian Journal of Statistics* **33**(1), 53–64.
- Durante, F. and Sempi, C. (2010), Copula theory: an introduction, in 'Copula theory and its applications', Springer, pp. 3–31.
- Falk, M. G., McGree, J. M. and Pettitt, A. N. (2014), 'Sampling designs on stream networks using the pseudo-Bayesian approach', *Environmental and Ecological Statistics* **21**(4), 751–773.
- Fuentes, M., Chaudhuri, A. and Holland, D. M. (2007), 'Bayesian entropy for spatial sampling design of environmental data', *Environmental and Ecological Statistics* **14**(3), 323–340.
- Genest, C. and MacKay, J. (1986), 'The joy of Copulas: bivariate distributions with uniform marginals', *The American Statistician* **40**(4), 280–283.
- Grler, B. and Pebesma, E. (2011), 'The pair-Copula construction for spatial data: a new approach to model spatial dependency', *Procedia Environmental Sciences* **7**, 206 – 211.
- Hill, W. J., Hunter, W. G. and Wichern, D. W. (1968), 'A joint design criterion for the dual problem of model discrimination and parameter estimation', *Technometrics* **10**(1), 145–160.
- Huang, Y., Hanneke, R. and Jones, R. (2019), 'Bibliometric analysis of cardiometabolic disorders studies involving  $NO_2$ ,  $PM_{2.5}$  and noise exposure', *BMC Public Health* **19**(1), 1–14.
- Joe, H. (2014), *Dependence Modeling with Copulas*, 1 edn, New York: Chapman and Hall/CRC.
- Kazianka, H. and Pilz, J. (2011), 'Bayesian spatial modeling and interpolation using Copulas', *Computers & Geosciences* **37**(3), 310 – 319.
- Kullback, S. and Leibler, R. A. (1951), 'On information and sufficiency', *The Annals of Math-*

- ematical Statistics* **22**(1), 79–86.
- Liu, J. and Vanhatalo, J. (2019), ‘Bayesian model based spatiotemporal survey designs and partially observed log Gaussian cox process’, *Spatial Statistics* **35**, 1–27.
- Long, Q., Scavino, M., Tempone, R. and Wang, S. (2013), ‘Fast estimation of expected information gains for Bayesian experimental designs based on Laplace approximations’, *Computer Methods in Applied Mechanics and Engineering* **259**, 24 – 39.
- McGree, J. M. (2017), ‘Developments of the total entropy utility function for the dual purpose of model discrimination and parameter estimation in Bayesian design’, *Computational Statistics and Data Analysis* **113**, 207–225.
- McGree, J. M., Eccleston, J. A. and Duffull, S. B. (2008), ‘Compound optimal design criteria for nonlinear models’, *Journal of Biopharmaceutical Statistics* **18**(4), 646–661.
- Meyer, R. K. and Nachtsheim, C. J. (1995), ‘The coordinate-exchange algorithm for constructing exact optimal experimental designs’, *Technometrics* **37**(1), 60–69.
- Müller, P., Sans, B. and Iorio, M. D. (2004), ‘Optimal bayesian design by inhomogeneous Markov chain simulation’, *Journal of the American Statistical Association* **99**(467), 788–798.
- Müller, W. (2007), *Collecting Spatial Data, 3rd revised and extended edition*, Springer Verlag, Heidelberg.
- Musafer, G. N. and Thompson, M. H. (2017), ‘Non-linear optimal multivariate spatial design using spatial vine Copulas’, *Stochastic Environmental Research and Risk Assessment* **31**(2), 551–570.
- Nelsen, R. (2006), ‘An introduction to Copulas, 2nd’, *New York: SpringerScience Business Media*.
- Overstall, A. M., McGree, J. M. and Drovandi, C. C. (2018), ‘An approach for finding fully Bayesian optimal designs using normal-based approximations to loss functions’, *Statistics and Computing* **28**(2), 343–358.
- Overstall, A. M. and Woods, D. C. (2017), ‘Bayesian design of experiments using approximate coordinate exchange’, *Technometrics* **59**(4), 458–470.
- Overstall, A. M., Woods, D. C. and Adamou, M. (2018), ‘acebayes: An R package for Bayesian optimal design of experiments via approximate coordinate exchange’, *arXiv:1705.08096*.
- Pilz, J., Schimek, M. and Spöck, G. (1997), Taking account of uncertainty in spatial covariance estimation, in ‘Geostatistics Wollongong 96’, Vol. 8, Kluwer Academic, pp. 302–313.
- Roberts, S., Arseneault, L., Barratt, B., Beevers, S., Danese, A., Odgers, C. L., Moffitt, T. E., Reuben, A., Kelly, F. J. and Fisher, H. L. (2019), ‘Exploration of  $NO_2$  and  $PM_{2.5}$  air pollution and mental health problems using high-resolution data in london-based children from a uk longitudinal cohort study’, *Psychiatry Research* **272**, 8–17.
- Sebastiani, P. and Wynn, H. P. (2000), ‘Maximum entropy sampling and optimal Bayesian experimental design’, *Journal of the Royal Statistical Society. Series B (Statistical Methodology)* **62**(1), 145–157.
- Tao, Y., Liu, J., Li, Z., Lin, J., Lu, T. and Yan, F. (2013), ‘Dose-finding based on bivariate efficacy-toxicity outcome using archimedean Copula’, *PLoS ONE* **8**(11), 1–6.

## Appendix

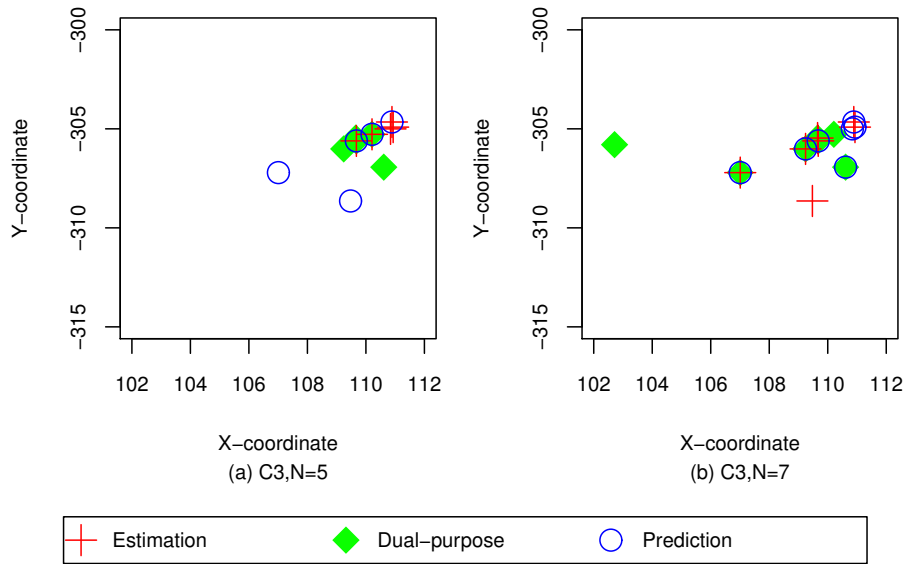


Figure 11: The optimal monitoring stations selected from C3 in Example 2 using each loss function

Table 6: Efficiencies of designs selected under each loss function from C3 in Example 2

Number of design points	Loss function	Estimation efficiency (%)	Prediction efficiency (%)
5	Estimation	100.00	80.62
	Dual-purpose	93.56	82.88
	Prediction	71.73	100.00
7	Estimation	100.00	82.03
	Dual-purpose	83.13	87.34
	Prediction	72.13	100.00

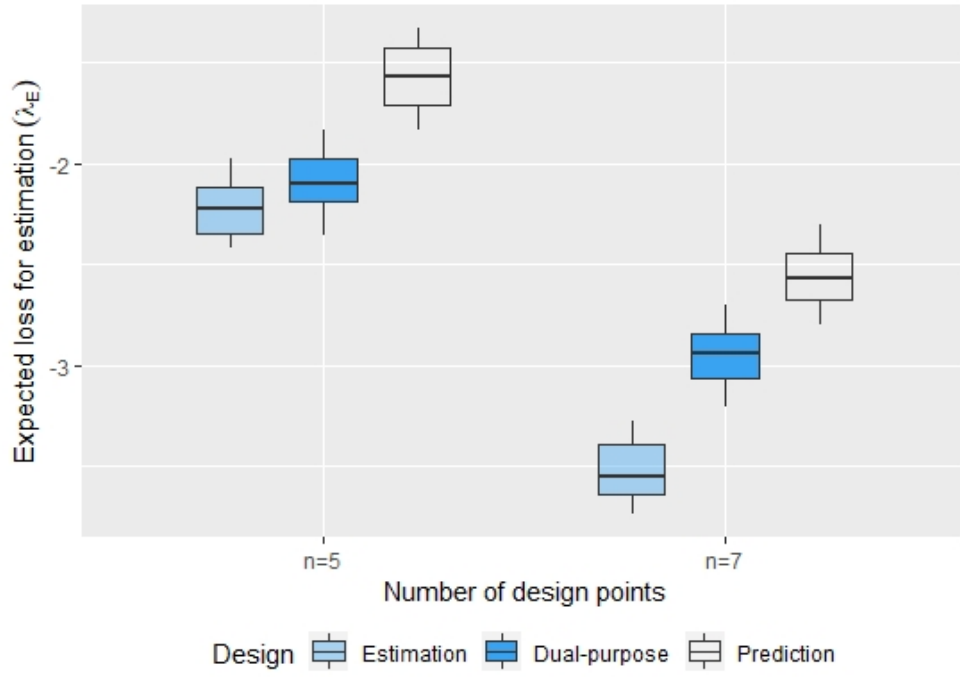


Figure 12: The boxplot of the distribution of the expected values for the loss function that focuses on parameter estimation for different designs over 50 simulations from C3 in Example 2

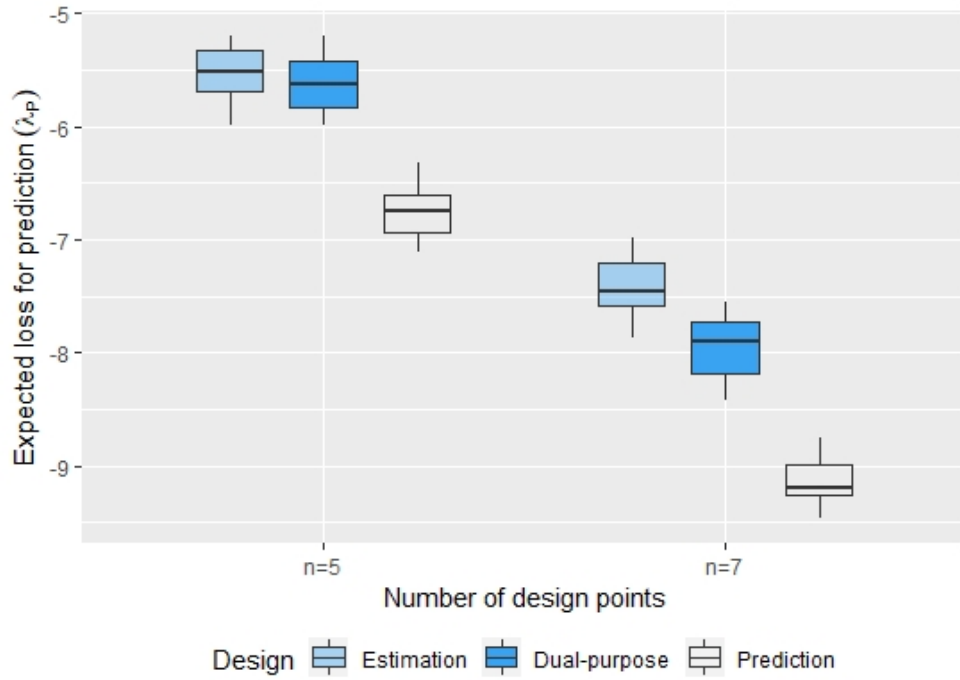


Figure 13: The boxplot of the distribution of the expected values for the loss function that focuses on prediction for different designs over 50 simulations from C3 in Example 2